


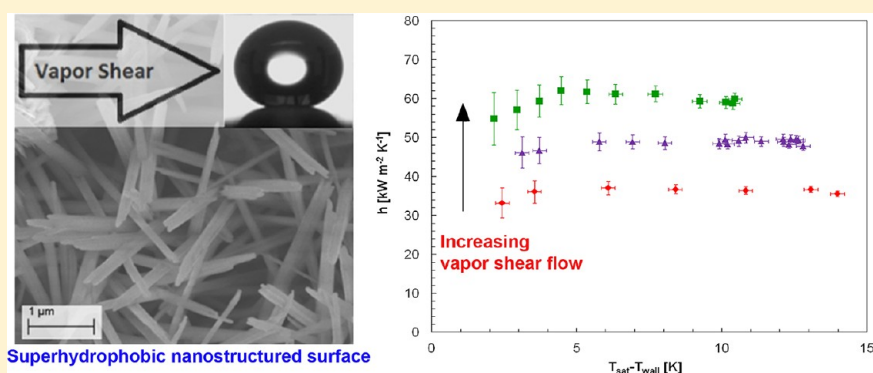
Flow Condensation on Copper-Based Nanotextured Superhydrophobic Surfaces

Daniele Torresin,^{†,‡,§} Manish K. Tiwari,^{*,†} Davide Del Col,[‡] and Dimos Poulikakos^{*,†}

[†]Laboratory of Thermodynamics in Emerging Technologies, Mechanical and Process Engineering Department, ETH Zurich, 8092 Zurich, Switzerland

[‡]Dipartimento di Ingegneria Industriale, Università degli Studi di Padova, 35131 Padova, Italy

 Supporting Information



ABSTRACT: Superhydrophobic surfaces have shown excellent ability to promote dropwise condensation with high droplet mobility, leading to enhanced surface thermal transport. To date, however, it is unclear how superhydrophobic surfaces would perform under the stringent flow condensation conditions of saturated vapor at high temperature, which can affect superhydrophobicity. Here, we investigate this issue employing “all-copper” superhydrophobic surfaces with controlled nanostructuring for minimal thermal resistance. Flow condensation tests performed with saturated vapor at a high temperature (110 °C) showed the condensing drops penetrate the surface texture (i.e., attain the Wenzel state with lower droplet mobility). At the same time, the vapor shear helped ameliorate the mobility and enhanced the thermal transport. At the high end of the examined vapor velocity range, a heat flux of $\sim 600 \text{ kW m}^{-2}$ was measured at 10 K subcooling and 18 m s^{-1} vapor velocity. This clearly highlights the excellent potential of a nanostructured superhydrophobic surface in flow condensation applications. The surfaces sustained dropwise condensation and vapor shear for five days, following which mechanical degradation caused a transition to filmwise condensation. Overall, our results underscore the need to investigate superhydrophobic surfaces under stringent and realistic flow condensation conditions before drawing conclusions regarding their performance in practically relevant condensation applications.

INTRODUCTION

Vapor condensation is an important phenomenon in nature and is directly relevant to many technical applications ranging from the chemical to the power industries. Enhancing thermal transport during condensation has been the subject of numerous scientific investigations. It is well-established that the dropwise condensation mode can lead up to a several hundred-percent enhancement in heat-transfer coefficients compared to that of film condensation.^{1,2} The sweeping and renewal mechanism present in the droplet growth process in dropwise condensation augments both the heat and mass transfer coefficients. On the other hand, during film condensation the liquid layer adjacent to the wall introduces an additional thermal resistance and adversely affects the thermal and mass transport. The surface properties, in particular the surface energy and the related phenomena, play a crucial role in determining the condensation mode. Typically,

hydrophobic surfaces are expected to promote dropwise condensation, while hydrophilic ones induce filmwise condensation.³ To this end, superhydrophobic surfaces, where a combination of low surface energy and surface texturing is used to enhance the hydrophobicity, have recently been proposed as a promising approach to promote dropwise condensation.^{4–7} An attractive feature of using superhydrophobic surfaces is to facilitate easy roll-off of the droplets as they form during condensation. Such facile mobility of the drops could lead to a significant improvement in the heat transfer associated with the condensation process.^{8–12} When condensation of humid air occurs, the mobility of droplets on superhydrophobic surfaces, however, is promoted by trapping air between the droplet and

Received: November 5, 2012

Revised: December 10, 2012

Published: December 19, 2012

the texture of the surface (i.e., by promoting the so-called Cassie state of a droplet on the superhydrophobic surface).¹³ The trapped air, although beneficial for droplet mobility, adds a thermal resistance, which adversely influences the thermal transport.¹⁴ During condensation of a pure vapor, it is assumed that the vapor trapped in the texture of the surface condenses in contact with the cold surface. Allowing the liquid to penetrate the asperities of the surface texture (i.e., by forming the so-called Wenzel state of the droplet) could at least partially ameliorate the thermal resistance problem. However, this leads to an increase in the droplet adhesion to the substrate and a corresponding reduction in droplet mobility. The increase in the droplet adhesion is also associated with an increase in the droplet contact angle hysteresis, which is the difference in the advancing and receding contact angles of the droplet. The Wenzel state with its high hysteresis is especially favored by a reduction in the liquid surface tension^{15,16} and increase in the ambient humidity.^{17,18} For practical applications, a high operation temperature, with the associated reduction in water surface tension, and saturated conditions are very relevant. Most of the previous reports on condensation experiments performed on superhydrophobic surfaces have focused on using the ideal environments of an environmental scanning microscope^{6,14,19–22} or condensation tests in unsaturated and room temperature conditions in the absence of any vapor shear flow.^{5,215,21} In addition, these works involve condensation of humid air (or gas). In our study, we deliberately avoided the presence of any noncondensable gases, which are known to affect condensation-based thermal transport across a solid surface. In addition, the majority of these studies have used top-down microfabrication as a means to obtain the nanotextured superhydrophobic surfaces. Recently, a novel approach was introduced, in which an immiscible liquid was impregnated into a nanotextured solid surface.²³ With carefully selected immiscible liquids, having desirable surface energy and spreading coefficient with respect to water, the authors reported remarkable increase in the mobility and decrease in the size of the shedding, condensed water droplets. These works have produced valuable results regarding drop formation and mobility, but only a few^{14,24} have actually focused on enhanced heat transfer rates. Miljkovic et al.¹⁴ showed that the “partial wetting” state of droplets (i.e., a state which is intermediate between the adhesive Wenzel and the mobile Cassie states)¹⁹ is best suited to improve thermal transport on superhydrophobic surfaces. On the other hand, Zhong et al.²⁴ reported an underperformance of a superhydrophobic oxidized copper surface compared to a mirror-polished one. The thermal resistance of the oxidized surface layer and degradation of polished metallic copper due to spontaneous oxidation (as is typical for metallic copper) can lead to substantial degradation in thermal properties of a substrate. To the best of our knowledge, no previous work has investigated the role of vapor flow on drop condensation on superhydrophobic surfaces. Apart from its obvious relevance in practical applications, the inherent unique feature of such flow condensation tests is that vapor shear can facilitate droplet mobility on a surface. In addition, as can be inferred from a broad body of classic literature dealing with flow condensation on nonsuperhydrophobic surfaces,^{25–28} it also augments thermal transport. A practical new challenge of using the vapor shear is the requirement of mechanical stability of the nanostructures in the surface texture when subjected to mechanical stress from the shear flow. Mechanical stability also influences the lifetime

of a surface in operation. These issues are directly addressed in this work through flow-condensation experiments on nano-engineered superhydrophobic copper surfaces. The experimental results are used to analyze the condensation mechanism, the thermal transport and the role of vapor flow rate thereof. The choice of copper as substrate and wet chemical nanotexturing is motivated by the prevalence of copper in real-life applications, which seek to exploit its high thermal conductivity. We use technically relevant test conditions of saturated vapor and high temperature (110 °C) during which penetration of droplet liquid interface into the surface texture occurs. This minimizes the thermal resistance. We then exploit the vapor shear effect to enhance the droplet mobility. A wet-chemical fabrication process was used to nanostructure the copper surfaces by oxidation and nanowire formation,²⁹ followed by surface functionalization to render them superhydrophobic. The surfaces were then evaluated using flow condensation tests at various vapor flow rates. The surfaces sustained dropwise flow condensation for five consecutive days of tests. This is an important first step for the potential viability of these nanostructured surfaces in practical applications, given that a polished copper sample got readily oxidized after only a day of exposure to our test conditions and showed filmwise condensation. Therefore, the nanotextured superhydrophobic surfaces demonstrate a 5-fold improvement in their lifetime with respect to sustenance of dropwise condensation compared to unprotected and uncoated copper. The approach also fares well in comparison to other state-of-the-art approaches for different applications. For example, very recently studied graphene coatings for dropwise condensation,³⁰ yielded a 7-fold improvement corrosion protection,³¹ and the corrosion protection offered by *n*-alkanethiol-based self-assembled monolayers is also known to degrade within a similar time frame.³² Overall, the present results indicate that whereas there are benefits to using nanotextured superhydrophobic samples in flow condensation applications, their durability under realistic conditions must be evaluated through long-term tests. This is apparent from their susceptibility to mechanical degradation due to shearing vapor flow and saturated conditions and temperature involved in flow condensation.

■ MATERIALS AND METHODS

Thermosyphon Flow Loop. A two-phase flow loop operating as thermosyphon was designed to study the condensation phenomenon and determine the heat-transfer coefficient. The vapor condensation tests were performed at a saturation temperature of 110 °C and pressure of 1.43 atm. Section I of the Supporting Information reports the details of the different flow-loop components and their control. Special care was taken to avoid any noncondensable gases, which could introduce errors in the measurement of heat transfer coefficients.² All tests were performed with DI water. For testing samples over consecutive days, the system was kept in overpressure overnight after nearly 10–12 h of sustained testing during the day.

Test Section. The minichannel test section was designed to measure the heat transfer coefficients during vapor flow condensation. The main part of the channel was made out of Teflon due to its high thermal stability and very low thermal conductivity ($0.23 \text{ W m}^{-1} \text{ K}^{-1}$), which helped ensure one-dimensional steady state heat conduction through the copper samples. The latter helped in accurate assessment of the heat transfer coefficients reported here. The minichannel was 22 mm wide and 2 mm high and had a length of 230 mm. A glass plate with built in heaters (to avoid vapor condensation and facilitate visualization) was used to cover the channel from the top. Each copper specimen had a nominal diameter of 20 mm and a length of 38 mm. On the side of the specimens opposite to the test surface (gray surface

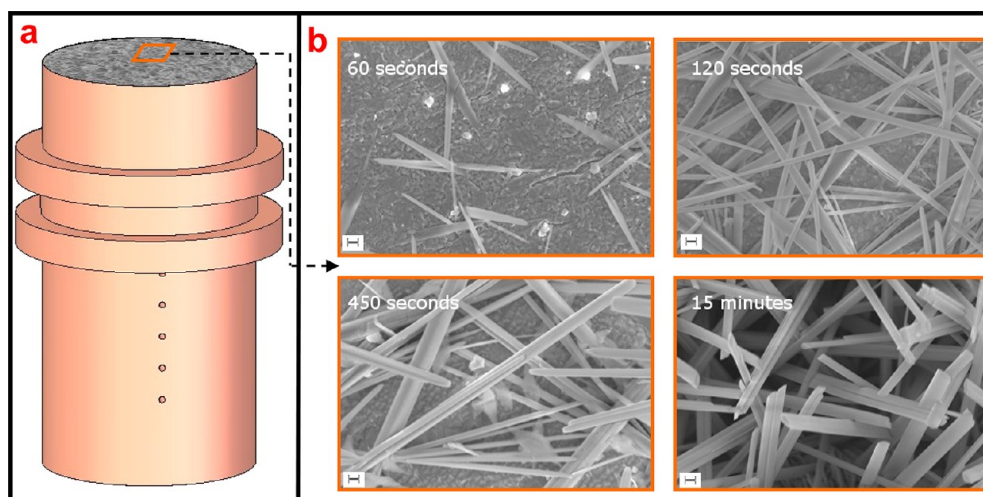


Figure 1. Test specimen and surface nanotexturing. (a) Schematic of the copper-made tested samples. The top (gray) surface of the sample was nanotextured and rendered superhydrophobic. (b) SEM images showing the development of the nanotexture with increase in solution immersion time. Each scale bar is 200 nm.

in Figure 1a), the copper specimens were in contact with a cooling system in order to dissipate the heat. The water bath 1 in Figure S1 of the Supporting Information was used for heat removal. The water flow rate was measured using an electromagnetic flow meter, while a thermocouple fitted to the inlet of the minichannel was used to measure the temperature. More details of the cooling system design are provided in Section II of the Supporting Information. Each copper specimen was fitted with 5 T-type thermocouples in precisely drilled holes into the sample specimens (see Figure 1a and Section III of the Supporting Information). The reported heat fluxes were determined from the slope of the measured temperature profile³³ (eq 1), and the average coefficient of condensation heat transfer was computed using the extrapolated specimen wall temperature (eq 2):

$$q = -k \frac{dT}{dz} \quad (1)$$

$$h = \frac{q}{T_{\text{sat}} - T_{\text{wall}}} \quad (2)$$

In eqs 1 and 2, k is the copper thermal conductivity, z is the axial position inside the cylindrical copper specimen, T_{sat} is the measured saturation temperature, and T_{wall} is the extrapolated surface temperature of the specimen where condensation takes place. For each heat flux measurement presented in the Results and Discussion, the flux calculated from eq 1 was compared with the one obtained from the energy balance of the cooling system. For the latter, the cooling water flow rate and temperature change were used to compute the caloric heat flux received by the water. For each data point reported (as a function of vapor flow rate and degree of supercooling), a minimum of 60 min was allowed in order to let the measured temperature stabilize and reach a steady-state condition. For lifetime testing, on each day the samples were subjected to a continuous testing for 10–12 h. Overnight, the flow loop was kept in overpressure in order to avoid any seepage of noncondensable gases. More details on the calibration process are presented in Section III of the Supporting Information.

Superhydrophobic Copper Sample Preparation. We used a wet chemical approach to develop the superhydrophobic surface,²⁹ in order to develop an “all-copper”, low-temperature surface treatment. The test surface of each copper specimen was first mechanically polished to a mirrorlike finish. Then, it was ultrasonically cleaned in ethanol (99% solvent grade) and Millipore DI water for 5 min each.

A two-step process was followed to form nanostructured superhydrophobic samples. First, the polished copper surface was immersed in a mixture solution containing 2.5 mol L⁻¹ sodium hydroxide (Merck) and 0.1 mol L⁻¹ ammonium persulphate (Sigma Aldrich) at room temperature for 12 min. The solution mixture was continuously

stirred with a magnetic stirrer during the entire immersion process. This step served to nanostructure the copper surface through a combination of oxidation and etching.²⁹ Subsequently, the surface was thoroughly rinsed with DI water and dried in a nitrogen stream. In the second step, to impart a surface energy change, a self-assembled monolayer was formed by a two-hour immersion of the nanostructured surface in an ethanol solution of 1H,1H,2H,2H-perfluorodecanethiol (Sigma Aldrich). The surface functionalization was performed at room temperature and followed by washing in ethanol for 1 h.

Contact Angle Measurement and Droplet Visualization. A Data Physics OCA20A system was used in the backlight configuration¹⁵ for contact angle measurements of 5 μ L droplets. The sliding angle measurements were performed by stage tilting and recording. The condensation process during each test was recorded with a Phantom V 9.1 high-speed camera. The videos were digitized into image sequences for analyzing the departing drop diameters with image processing.

RESULTS AND DISCUSSION

Surface Characterization. The scanning electron microscope (SEM) images shown in Figure 1b capture the surface morphology of the samples obtained by varying the immersion time during the first step. As reported first by Chen et al.,²⁹ clearly the oxidation and etching lead to formation of Cu(OH)₂ nanowires, which gradually cover the entire surface of the copper substrate. The nanowires are crucial to the formation of the rough superhydrophobic surface. However, the thermal conductivity of Cu(OH)₂ is 1 order of magnitude lower than that of copper. Therefore, it was important to find the optimal solution immersion time that yielded superhydrophobicity with minimal degradation in the substrate thermal resistance due to the increased thickness of the Cu(OH)₂ nanowire layer. Clearly, the nanostructuring is rapid and after only 30 s, some nanowires already appear in the surface. Increasing the immersion time results in an increase of the nanowire length and in uniformity of the surface coverage. After 15 min the surface is uniformly covered with nanowires whose length is almost the same as at 450 s.

At the end of the optimization step, a 12 min immersion time was found sufficient for complete surface coverage with a layer of nanowires and also resulted in a superhydrophobic sample behavior (see the next subsection) after functionalization.

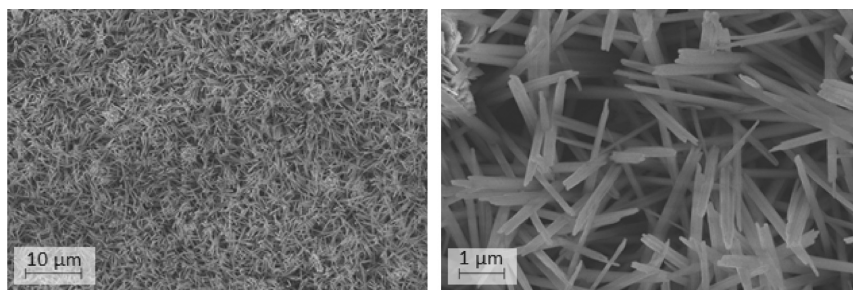


Figure 2. SEM images of the copper surface structures at a 12 min immersion time.

Figure 2 shows the morphology of the resulting surface. Determining the optimal immersion time was also crucial for the mechanical durability of the nanostructured surfaces. In fact, a surface immersion time of 20 min led to a fragile nanowire layer, which could readily be removed through gentle rubbing of the surface. Mechanical strength is crucial for stability against vapor shear, which is the main focus of the current work. The nanowire layer with 12 min immersion had sufficient mechanical strength to easily withstand the range of vapor shear rates tested here.

Contact Angle Measurements. The initial polished copper surface was hydrophilic with a contact angle of $86 \pm 2^\circ$ (Figure 3a). The contact angle changed significantly upon

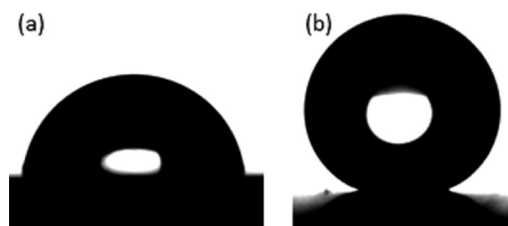


Figure 3. Change in wettability with nanostructuring and functionalization. Water droplets ($5 \mu\text{L}$) on (a) the initial polished copper sample and (b) the nanostructured and functionalized superhydrophobic copper sample.

nanostructuring. Before surface functionalization, the nanostructured samples exhibited a contact angle less than 5° , characteristic of superhydrophilic surfaces. However, after the functionalization with the fluorosilane, the surface free energy of the samples was reduced drastically resulting in a contact angle of $159^\circ \pm 2^\circ$ (Figure 3b) and a sliding angle of less than 2° . The latter is the resolution of the stage used for the sliding angle measurement since it was nearly impossible to place a droplet on the surface without it rolling off.

Velocity Characterization. In our setup, the vapor mass flow rate could be adjusted by changing the electrical power supplied to the boiling chamber. A fine regulation of the needle valve enabled the control on the vapor flow and its stabilization. The vapor mass flow rate can be obtained from an energy balance of the boiling chamber as

$$\dot{m}_{\text{vapor}} = \frac{Q_{\text{bc}}}{(h_{\text{L,sat}} - h_{\text{L,sub}}) + h_{\text{LV}}} \quad (3)$$

where $h_{\text{L,sat}}$ and $h_{\text{L,sub}}$ are the enthalpies of saturated and subcooled water at the respective temperature and pressure measured at the boiling chamber inlet and h_{LV} is the corresponding latent heat of vaporization. In eq 3, Q_{bc} is the electric power supplied to the boiling chamber, which was

measured with a NORMA AC Power Analyzer D 5255 S. The above-calculation neglects the heat losses to the ambient air in the part of the flow loop extending from the boiling chamber to the test section. This is justified given the fact that we used good foam insulation. A simple estimation of the heat losses using the correlation for natural convection yields a heat loss of $\sim 2\%$, thus justifying our approach to neglect the heat loss, while calculating the vapor mass flow rate and velocity. A detailed error analysis for the heat-flux and heat-transfer coefficient measurements are provided in Section VI of the Supporting Information.

The test section was vertically oriented with a downward vapor flow. Therefore, in our setup, the vapor shear and the gravitational forces acted together to aid condensate droplet removal. The gravity effect plays a role in droplet removal only if the drop diameter is comparable to the liquid capillary length³⁴

$$\kappa^{-1} = \sqrt{\frac{\sigma_{\text{LV}}}{\rho_{\text{V}}g}} \quad (4)$$

where σ_{LV} is the water surface tension, ρ_{L} is the condensate density, and g is the acceleration due to gravity. For water at 1.43 bar (i.e., the test condition in our experiments), the capillary length comes out to be 2.45 mm. The size of departing droplets on nanotextured superhydrophobic surfaces was approximately millimeters; therefore, in our experiments both gravity and the vapor shear induce the droplet mobility on the surfaces.

Influence of Vapor Shear Rate. The influence of the vapor shear on nanostructured superhydrophobic copper surfaces was analyzed first. The saturated vapor entered the test section at a controlled temperature of 110°C . The temperature of the superhydrophobic copper surface was tuned by varying the inlet conditions in the cooling water system on the back side of the samples. Figures 4 and 5 show the variation of heat flux, q , and the heat transfer coefficient, h , with the degree of solid surface subcooling (i.e., the difference between the water saturation and the solid surface temperatures). To ensure the accuracy of the results for each measurement, the error bars were calculated from a detailed uncertainty analysis described in Section VI of the Supporting Information. Note the error bars in heat flux measurements are too small to be visible. For each data point, first the agreement between the calculated (from the measured pressure) and the directly measured saturation temperatures (at the test section inlet) was checked. The measurements were recorded only if the disagreements were within the measurement uncertainty. Once the agreement was verified, the steady-state conditions were reached within ~ 1 h. Three different vapor shear rates were tested with vapor velocities of 6, 12, and 18 m s^{-1} . For all

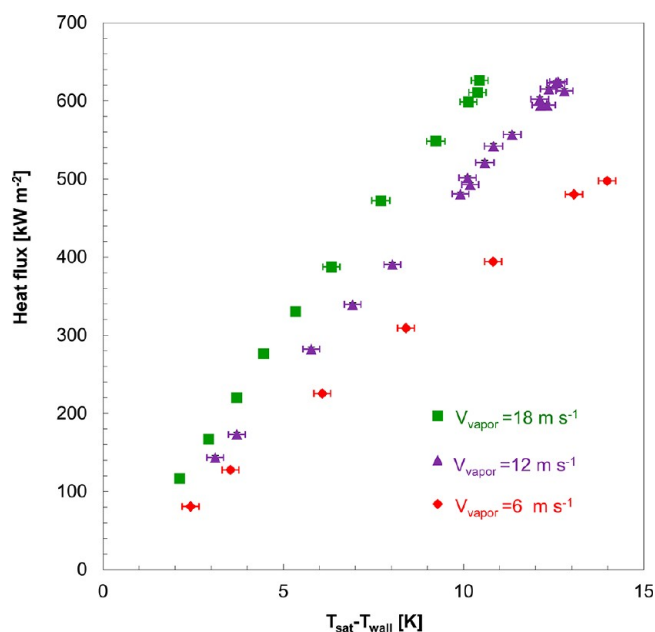


Figure 4. Heat flux as a function of wall subcooling during DWC on the superhydrophobic copper sample at three different vapor velocities.

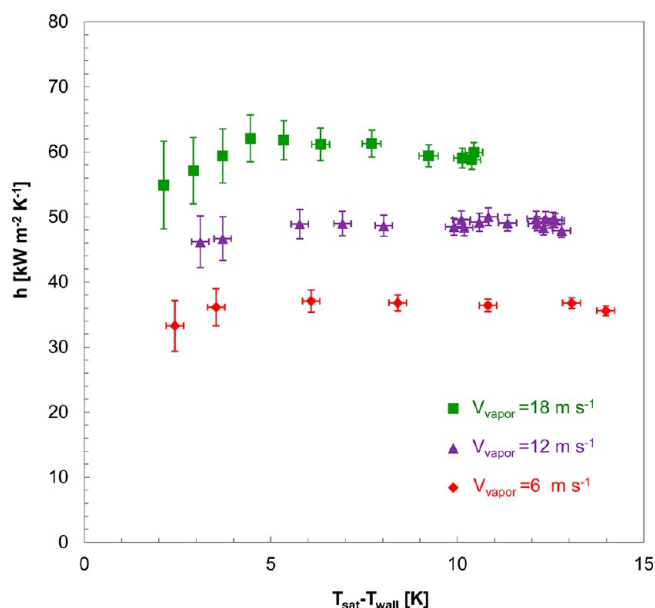


Figure 5. Heat transfer coefficient dependence on the wall subcooling during DWC on a superhydrophobic copper sample at three different vapor velocities.

these measurements, vapor condensed on the nanostructured surfaces in the dropwise mode. As shown in Figure 4, the heat flux increases both with an increase in the wall subcooling and the flow rate. This is due to the reduction in the size of the departing droplets with an increase in the flow rate. The vapor shear imposes a drag force on a condensing droplet. When the drag overcomes the capillary adhesion of the droplet on the surface, the droplet will move. A simple scaling analysis for this concept is discussed in more detail in Section IV of the Supporting Information. Clearly, the increase in the shear rate should result in a reduction in the departing droplet size, thereby increasing the rate of thermal transport.^{8,25}

The heat-transfer coefficient exhibits a different behavior: it remains rather insensitive (in particular at higher subcooling) to increases in subcooling and seems to depend strongly on the vapor velocity (Figure 5). The latter finding clearly underpins the beneficial influence of vapor velocity on the thermal performance of the nanostructured surfaces. Note that in our measurements, the benefits of the vapor velocity are not easily quantifiable at subcooling below 3 K, where the measurements for different vapor velocities display larger measurement error bars.

Lifetime Test. In order to test their mechanical and chemical robustness, the nanostructured superhydrophobic copper samples were tested for several days. In Figure 6, the

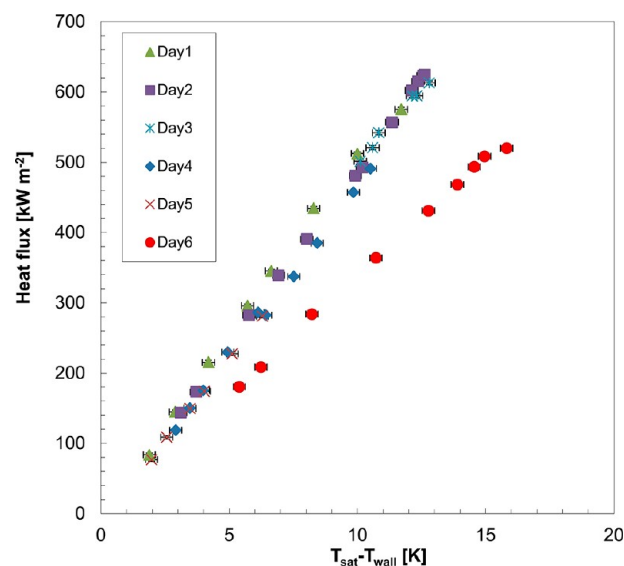


Figure 6. Thermal performance of a nanostructured superhydrophobic copper sample over 6 consecutive days of condensation tests at 110 °C and 12 m s⁻¹ vapor velocity. The condensation mode switched from dropwise to filmwise on the sixth day.

heat flux as a function of the wall subcooling is shown for measurements performed over six consecutive days. All the measurements in the figure were obtained at a saturation temperature of 110 °C (1.43 atm) and a vapor velocity of 12 m s⁻¹. For the first five days, there are no signs of degradation in the surface performance and the heat flux values are reproduced at different degrees of subcooling. A clear difference in the heat flux trend is observed on the sixth day: at the same subcooling conditions the heat flux is reduced by 35% with respect to the previous days. This is explained by the change in the mode of condensation, resulting in the surface almost entirely being covered by a film of the condensate. The decrease in the thermal performances appears to be the result of the deterioration of the hydrophobic monolayer³⁵ combined with the gradual mechanical degradation of the surface (see SEM images in Figure 7). The latter effect results from the sustained exposure to measurement temperatures up to ~110 °C and high vapor velocity. Figure 7 shows the SEM images, at two different magnifications, of the sample after five days of testing. A comparison of the surface morphology in Figure 7 with the ones reported before in Figure 2, the surface degradation is clear. In fact, after the sustained tests, although some nanotexturing does seem to remain, there is no sign of the nanowires.

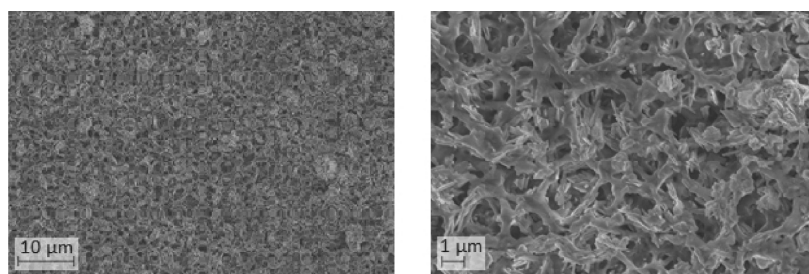


Figure 7. Low and high magnification SEM images of the superhydrophobic copper sample after five days of experiments.

Comparison with Nontextured Copper. For comparison purposes, tests were also performed on a nontextured oxidized copper surface. To obtain oxidized copper surfaces, cleaned, mirror-polished copper samples were fitted into the test section and exposed to a sustained vapor flow of 12 m/s at $\sim 110^\circ\text{C}$ temperature. After several hours of exposure, the color of the sample changed and gradually the mode of vapor condensation switched to filmwise condensation. This is expected given the fact that copper is susceptible to oxidation and corrosion, which makes the surface treatment worthwhile in the first place. The heat flux in filmwise mode on the oxidized, nontextured copper sample was recorded only after the measured temperatures stabilized, which happened after a day of exposure to the present test conditions. The corresponding heat flux variation on the oxidized, polished copper with filmwise condensation and a nanotextured superhydrophobic sample with dropwise condensation are plotted in Figure 8. The reason to compare

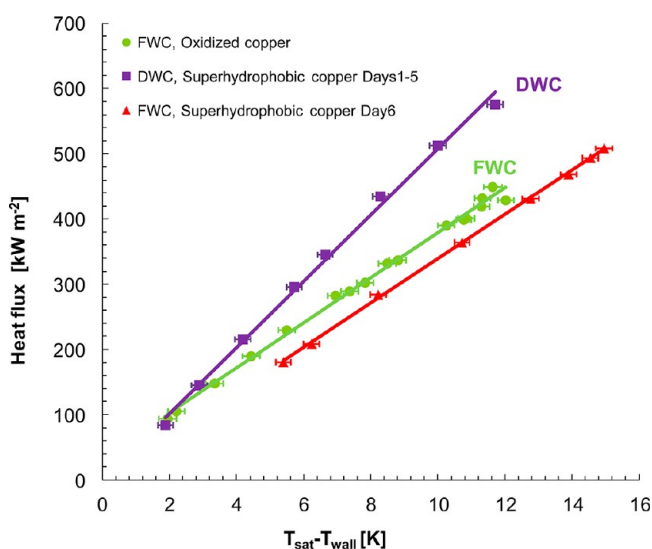


Figure 8. Comparison of the heat fluxes during condensation on a nanotextured superhydrophobic and a naturally oxidized polished copper sample. Both the measurements were performed at a saturation temperature of 110°C and a vapor velocity of 12 m s^{-1} .

the filmwise condensation on pure copper with dropwise condensation on nanostructured copper sample is to show the expected advantage of using nanostructured surfaces as opposed to the polished copper, which only sustained dropwise condensation for several hours and at most for a day of tests. The lines are data fits. The figure shows data for days 1–5 and 6 for the superhydrophobic sample. Note that since the measurements on the first 5 days were nearly overlapping with each other (see the above discussion in the context of Figure

6), we only show the data for day 1 in Figure 8 and label it as day 1–5. Clearly, for the first five days of tests under the same operation conditions (vapor velocity and pressure), the thermal performance of the superhydrophobic sample is better than the oxidized copper sample. At subcooling below 3 K, the two surfaces display no differences in the heat flux values. However, with a decrease in the surface temperature, the superior performance of the superhydrophobic, nanostructured surface becomes clear. This is due to the increase of the condensate layer thickness, which causes an augmentation of the thermal resistance and so a decrease in the thermal transport in film condensation. In addition, a heat flux as high as 600 kW m^{-2} is measured with 10 K subcooling on the nanotextured superhydrophobic surface (see Figure 4), which is comparable to the values reported in the literature on nontextured functionalized surfaces.²⁴ The five days of sustained dropwise condensation on superhydrophobic nanostructured samples shows an encouraging first result in terms of the potential application of these surfaces in intense flow condensation applications, which are practically most relevant. The polished copper surfaces degraded after only a day due to oxidation. This result shows a nearly 5-fold improvement in the lifetime of stable dropwise condensation on nanostructured copper surfaces as compared to that on the untreated copper. In Figure 8, we report the measurements on the superhydrophobic sample on day 6, which clearly show degradation in the thermal performance. Visual observations confirmed that this coincided with switching the condensation mode to film condensation. Note also that an as-prepared surface, without being subjected to a condensation test, showed no degradation in the superhydrophobicity, even after a shelf storage of over 6 months (tested through contact angle and sliding angle measurements). This shows that practically relevant flow condensation testing under saturated conditions at high temperature can degrade an apparently robust superhydrophobic surface (see Figure 7). Therefore, while developing improved methods and coatings for condensation enhancement is needed and should be encouraged, the longer-term flow condensation performance under realistic conditions must be studied in parallel. This will help place the results into proper perspective, before novel superhydrophobic surfaces, or for that matter any surface treatment, could be hailed as an exceptional and robust means for promotion of dropwise condensation.

It is also important to point out that thermal performance of oxidized copper becomes better than the superhydrophobic surface after day 6 (see Figure 8). The reason for this is the higher thermal resistance of the nanostructured superhydrophobic surface compared to the nontextured oxidized copper surface.

Visualization and Analysis of Dropwise Condensation. The digitized image sequences from high-speed video

recording of the condensation process were used to gain insight into the condensation process on the nanostructured superhydrophobic copper samples. The image sequence shown in the Figure 9 captures the dropwise condensation on a sample

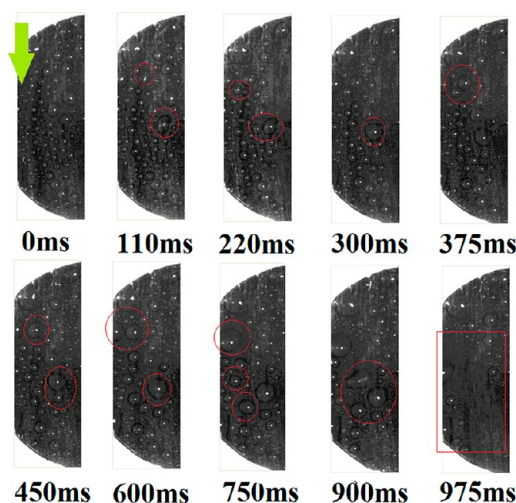


Figure 9. Droplet cycle on a superhydrophobic copper sample at 2 K of surface subcooling and a vapor velocity of 12 m s^{-1} . The arrow indicates the vapor flow direction.

subjected to a vapor velocity of 12 m s^{-1} and a subcooling of 2 K. The condensation process was found to be cyclic in nature, characterized by drop nucleation, growth, and departure. The cyclic condensation process was observed to repeat itself with a frequency that depended upon the surface temperature and the vapor velocity. The cycle started with nucleation of small droplets (0 ms), which grew and coalesced together with time due to continuous vapor condensation. During coalescence the center of mass of the merging drops did not change appreciably before and after coalescence (110–900 ms). After growing to a critical diameter, drops became mobile (900–975 ms) and departed downstream (top to bottom in the images shown in Figure 9). The departing drops swept over the surface, thereby wiping small droplets in their path. After the drop sweep, fresh drops started to nucleate (975 ms) and grow, allowing the cyclic process to continue.

The effect of the vapor shear rate during DWC is highlighted in Figure 10, which shows the difference in the condensation

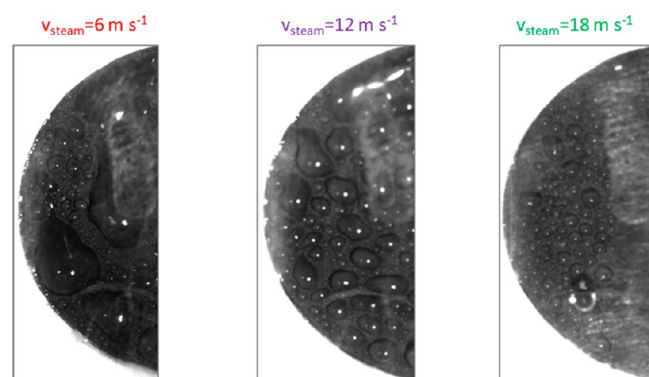


Figure 10. Effect of vapor shear velocity on droplet size during DWC on a superhydrophobic copper sample. Surface subcooling was 3.5 K. A video of the phenomenon at 18 m s^{-1} is provided in the Supporting Information.

process on the superhydrophobic copper sample at the same surface subcooling of 3.5 K but at three different vapor shear velocities of 6, 12, and 18 m s^{-1} . Clearly, with an increase in the vapor velocity, the size of the departing droplets becomes smaller (c.f. explanation in Section IV of the Supporting Information). A close inspection and analysis of the high-speed videos of the tests in Figure 10, it was observed that the droplet departure frequency was also observed to increase with vapor shear. It is well-established in the literature that even at equal surface coverage, the heat transfer rate increases with a decreasing average departing drop diameter.^{2,36} This is due to the lower thermal resistance of the smaller drops. Therefore, it becomes obvious that increasing the vapor velocity, with the resulting decrease in the drop departure diameter, contributes to enhance the thermal performance surfaces (see Figures 4 and 5).

For further insight into the experimental results presented above, we note that in our test conditions of 110°C , the water surface tension is $\sim 56 \text{ mN/m}$.³⁷ In addition, our experiments are performed with pure vapor in saturated conditions. Both these facts (low surface tension^{15,16} and saturation^{17,18}) are known to favor the Wenzel state of droplets on superhydrophobic surfaces, which is characterized by the liquid meniscus penetrating the surface texture. The recent literature concerning the use of superhydrophobic surfaces has mostly focused on experiments with the environmental scanning microscope^{6,14,19–22} and/or condensation tests in the absence of external flow, performed in unsaturated and room temperature conditions.^{5,21} Water surface tension in these studies should be 72 mN/m or higher, reaching as high as 76 mN/m in the conditions used in reference 14, thereby favoring the Cassie state and its associated droplet mobility. However, the thermal resistance could undesirably increase, due to the gas/vapor trapped underneath the droplets in the Cassie state. To this end, the Wenzel state with its associated liquid penetration into the surface asperities is beneficial to the thermal transport, since it avoids the thermal resistance of the trapped gas. The current work is the first attempt at using a scalable, all-copper-based nanoengineered superhydrophobic surface under realistic and intensive condensation conditions and evaluating the simultaneous effect of vapor shear velocity on dropwise condensation and thermal transport. We refer to our approach as scalable, in order to indicate that the wet chemical approach used for nanostructuring can easily be applied to larger size surfaces than those used in our study. The results clearly indicate that nanotextured superhydrophobic surfaces should be evaluated through prolonged flow condensation tests, due to their vulnerability to mechanical degradation under vapor shear flow.

CONCLUSIONS

In conclusion, we report the results of flow condensation experiments on nanoengineered superhydrophobic all-copper surfaces. A wet-chemical fabrication process was used to nanotexture a copper surface by forming nanowires; the resulting surface was superhydrophilic. Surface functionalization introduced superhydrophobicity to the surfaces. The resulting superhydrophobic samples showed a high contact angle of 159° and a nearly zero sliding angle at room temperature. Thermal performances of superhydrophobic nanostructured copper and oxidized polished copper samples were compared via flow condensation tests at a 110°C saturation temperature. The high temperature and saturated vapor caused the condensate droplets on the superhydrophobic surfaces to primarily appear

in the Wenzel state. However, the vapor-induced shear forces could clearly improve droplet mobility and reduce the critical size of the departing droplets, thereby enhancing the thermal transport on the nanostructured superhydrophobic surfaces. A heat flux of $\sim 600 \text{ kW m}^{-2}$ was recorded for a vapor shear velocity of 18 ms^{-1} at 10 K wall subcooling. The superhydrophobic samples sustained dropwise condensation for five days of testing. Overall, the present results indicate that, while using superhydrophobicity concepts to develop novel coatings and surfaces for enhanced condensation applications is worthwhile and should indeed be promoted, heralding the superior performance of such surfaces must be preceded by flow condensation tests in realistic high temperature and saturation conditions.

■ ASSOCIATED CONTENT

Supporting Information

Detailed description of the thermosyphon flow loop, test section, surface temperature determination, drop size dependence on vapor velocity, measurement sensors, uncertainty estimation procedure, and a video showing the shedding of condensed droplets. This material is available free of charge via the Internet at <http://pubs.acs.org>.

■ AUTHOR INFORMATION

Corresponding Authors

*M.K.T.: e-mail, mtiwari@ethz.ch.

*D.P.: e-mail, dpoulidakos@ethz.ch.

Present Address

[§]ABB Schweiz AG, Segelhofstrasse 1K, 5405, Baden-Daettwil, Aargau, Switzerland.

Author Contributions

All authors were involved in problem conception. D.T. designed the experimental setup, prepared the surfaces, and performed the measurements with direct input and mentoring by M.K.T. D.P. and D.D.C. provided overall guidance for all the scientific elements of the research. All authors participated in writing the paper and discussion of the results.

Notes

The authors declare no competing financial interest.

■ ACKNOWLEDGMENTS

We gratefully acknowledge financial support from the Eng. Aldo Gini fellowship. The authors thank Anja Huch (EMPA, Zurich) for help with the contact angle measurements, Tobias Bachmann (LTNT student, ETH Zurich) for the SEM images, and Peter Kocher (MATL, ETH Zurich) for the surface polishing.

■ ABBREVIATIONS

SEM: Scanning Electron Microscope; DWC: dropwise condensation; FWC: filmwise condensation

■ REFERENCES

- (1) Schmidt, E.; Schurig, W.; Sellschopp, W. Versuche über die kondensation von wasserdampf in film: und tropfenform. *Forsch. Ingenieurwes.* **1930**, *1* (2), 53–63.
- (2) Rose, J. W. Dropwise condensation theory and experiment: A review. *Proc. Inst. Mech. Eng., Part A* **2002**, *216* (2), 115–128.
- (3) Rainieri, S.; Bozzoli, F.; Pagliarini, G. Effect of a hydrophobic coating on the local heat transfer coefficient in forced convection under wet conditions. *Exp. Heat Transfer* **2009**, *22* (3), 163–177.

- (4) Chen, C.-H.; Cai, Q.; Tsai, C.; Chen, C.-L.; Xiong, G.; Yu, Y.; Ren, Z. Dropwise condensation on superhydrophobic surfaces with two-tier roughness. *Appl. Phys. Lett.* **2007**, *90* (17), 173108.
- (5) Boreyko, J. B.; Chen, C.-H. Self-Propelled dropwise condensate on superhydrophobic surfaces. *Phys. Rev. Lett.* **2009**, *103* (18), 184501.
- (6) Dietz, C.; Rykaczewski, K.; Fedorov, A. G.; Joshi, Y. Visualization of droplet departure on a superhydrophobic surface and implications to heat transfer enhancement during dropwise condensation. *Appl. Phys. Lett.* **2010**, *97* (3), 033104.
- (7) Kim, S.; Kim, K. J. Dropwise condensation modeling suitable for superhydrophobic surfaces. *J. Heat Transfer* **2011**, *133* (8), 081502.
- (8) Graham, C.; Griffith, P. Drop size distributions and heat transfer in dropwise condensation. *Int. J. Heat Mass Transfer* **1973**, *16* (2), 337–346.
- (9) Dorrer, C.; Rühe, J. Condensation and wetting transitions on microstructured ultrahydrophobic surfaces. *Langmuir* **2007**, *23* (7), 3820–3824.
- (10) Narhe, R. D.; Beysens, D. A. Nucleation and growth on a superhydrophobic grooved surface. *Phys. Rev. Lett.* **2004**, *93* (7), 076103.
- (11) Varanasi, K. K.; Hsu, M.; Bhate, N.; Yang, W.; Deng, T. Spatial control in the heterogeneous nucleation of water. *Appl. Phys. Lett.* **2009**, *95* (9), 094101.
- (12) Feng, J.; Qin, Z.; Yao, S. Factors affecting the spontaneous motion of condensate drops on superhydrophobic copper surfaces. *Langmuir* **2012**, *28* (14), 6067–6075.
- (13) Lafuma, A.; Quere, D. Superhydrophobic states. *Nat. Mater.* **2003**, *2* (7), 457–460.
- (14) Miljkovic, N.; Enright, R.; Wang, E. N. Effect of droplet morphology on growth dynamics and heat transfer during condensation on superhydrophobic nanostructured surfaces. *ACS Nano* **2012**, *6* (2), 1776–1785.
- (15) Tiwari, M. K.; Bayer, I. S.; Jursich, G. M.; Schutzius, T. M.; Megaridis, C. M. Highly liquid-repellent, large-area, nanostructured poly(vinylidene fluoride)/poly(ethyl 2-cyanoacrylate) composite coatings: Particle filler effects. *ACS Appl. Mater. Interfaces* **2010**, *2* (4), 1114–1119.
- (16) Yuyang, L.; Xianqiong, C.; Xin, J. H. Can superhydrophobic surfaces repel hot water? *J. Mater. Chem.* **2009**, *19* (31), S602–S611.
- (17) Yin, L.; Zhu, L.; Wang, Q.; Ding, J.; Chen, Q. Superhydrophobicity of natural and artificial surfaces under controlled condensation conditions. *ACS Appl. Mater. Interfaces* **2011**, *3* (4), 1254–1260.
- (18) Jung, S.; Tiwari, M. K.; Doan, N. V.; Poulidakos, D. Mechanism of supercooled droplet freezing on surfaces. *Nat. Commun.* **2012**, *3*, Article number 615, DOI: <http://dx.doi.org/10.1038/ncomms1630>.
- (19) Rykaczewski, K.; Scott, J. H. J. Methodology for imaging nano-to-microscale water condensation dynamics on complex nanostructures. *ACS Nano* **2011**, *5* (7), 5962–5968.
- (20) Rykaczewski, K.; Scott, J. H. J.; Rajauria, S.; Chinn, J.; Chinn, A. M.; Jones, W. Three dimensional aspects of droplet coalescence during dropwise condensation on superhydrophobic surfaces. *Soft Matter* **2011**, *7* (19), 8749–8752.
- (21) Chen, X. M.; Wu, J.; Ma, R. Y.; Hua, M.; Koratkar, N.; Yao, S. H.; Wang, Z. K. Nanograsped micropylamidal architectures for continuous dropwise condensation. *Adv. Funct. Mater.* **2011**, *21* (24), 4617–4623.
- (22) Rykaczewski, K.; Landin, T.; Walker, M. L.; Scott, J. H. J.; Varanasi, K. K. Direct imaging of complex nano- to microscale interfaces involving solid, liquid, and gas phases. *ACS Nano* **2012**, *6* (10), 9326–9334.
- (23) Anand, S.; Paxson, A. T.; Dhiman, R.; Smith, J. D.; Varanasi, K. K. Enhanced condensation on lubricant-impregnated nanotextured surfaces. *ACS Nano* **2012**, *6*, 10122–10129.
- (24) Zhong, L.; Xuehu, M.; Sifang, W.; Mingzhe, W.; Xiaonan, L. Effects of surface free energy and nanostructures on dropwise condensation. *Chem. Eng. J. (Amsterdam, Neth.)* **2010**, *156* (3), 546–552.

- (25) Tanasawa, I.; Utaka, Y. Measurement of condensation curves for dropwise condensation of steam at atmospheric-pressure. *J. Heat Transfer* **1983**, *105* (3), 633–638.
- (26) Tanasawa, I.; Ochiai, J.-I. Experimental study on dropwise condensation. *Bull. JSME* **1973**, *16* (98), 1184–1197.
- (27) Takeyama, T.; Shimizu, S. On the transition of dropwise-film condensation. *Heat Transfer* **1974**, *3*, 274–278.
- (28) Yamali, C.; Merte, H., Jr. Influence of sweeping on dropwise condensation with varying body force and surface subcooling. *Int. J. Heat Mass Transfer* **1999**, *42* (15), 2943–2953.
- (29) Chen, X.; Kong, L.; Dong, D.; Yang, G.; Yu, L.; Chen, J.; Zhang, P. Synthesis and characterization of superhydrophobic functionalized Cu(OH)₂ nanotube arrays on copper foil. *Appl. Surf. Sci.* **2009**, *255* (7), 4015–4019.
- (30) Rafiee, J.; Mi, X.; Gullapalli, H.; Thomas, A. V.; Yavari, F.; Shi, Y. F.; Ajayan, P. M.; Koratkar, N. A. Wetting transparency of graphene. *Nat. Mater.* **2012**, *11* (3), 217–222.
- (31) Prasai, D.; Tuberquia, J. C.; Harl, R. R.; Jennings, G. K.; Bolotin, K. I. Graphene: Corrosion-inhibiting coating. *ACS Nano* **2012**, *6* (2), 1102–1108.
- (32) Laibinis, P. E.; Whitesides, G. M. Self-assembled monolayers of *n*-alkanethiolates on copper are barrier films that protect the metal against oxidation by air. *J. Am. Chem. Soc.* **1992**, *114* (23), 9022–9028.
- (33) Del Col, D.; Webb, R. L.; Narayanamurthy, R. Heat transfer mechanisms for condensation and vaporization inside a microfin tube. *J. Enhanced Heat Transfer* **2002**, *9* (1), 25–37.
- (34) De Gennes, P. G.; Brochard-Wyart, F.; Quéré, D., *Capillarity and Wetting Phenomena: Drops, Bubbles, Pearls, Waves*. Springer: New York, 2004.
- (35) Fréchette, J.; Maboudian, R.; Carraro, C. Thermal behavior of perfluoroalkylsiloxane monolayers on the oxidized Si(100) surface. *Langmuir* **2006**, *22* (6), 2726–2730.
- (36) Rose, J. W.; Glicksman, L. R. Dropwise condensation—The distribution of drop sizes. *Int. J. Heat Mass Transfer* **1973**, *16* (2), 411–425.
- (37) Vargaftik, N. B.; Volkov, B. N.; Voljak, L. D. International tables of the surface-tension of water. *Journal of Physical Chemistry Reference Data* **1983**, *12* (3), 817–820.